Supporting Information

Low-overpotential rechargeable Na-CO_2 batteries enabled by an oxygen-vacancy-rich cobalt oxide catalyst

*Zhi Zheng [ab], Xiaobo Zheng [a], Jicheng Jiang [a], Qi Zhang [a], Peng Li [c], Can Li *[d], Qinfen Gu [e], Li Wei [b], Konstantin Konstantinov [a], Weishen Yang [f], Yuan Chen *[b], Jiazhao Wang *[ag]*

a Institute for Superconducting and Electronic Materials, University of Wollongong, North Wollongong, New South Wales 2500, Australia.

b School of Chemical and Biomolecular Engineering, The University of Sydney, Darlington, New South Wales 2006, Australia.

c School of Science, RMIT University, Melbourne, Victoria 3000, Australia

d College of Optoelectronic Materials and Devices, China Jiliang University, Hangzhou 310018, China.

e The Australian Synchrotron (ANSTO), 800 Blackburn Road, Clayton, Victoria 3168, Australia.

f State Key Laboratory of Catalysis, Dalian Institute of Chemical Physics, Chinese Academy of Sciences, 457 Zhongshan Road, Dalian 116023,China.

g Institute for Carbon Neutralization, College of Chemistry and Materials Engineering, Wenzhou University, Wenzhou, 325035, China

*Corresponding authors

Email: canli@cjlu.edu.cn

Email: yuan.chen@sydney.edu.au

Email: jiazhao@uow.edu.au

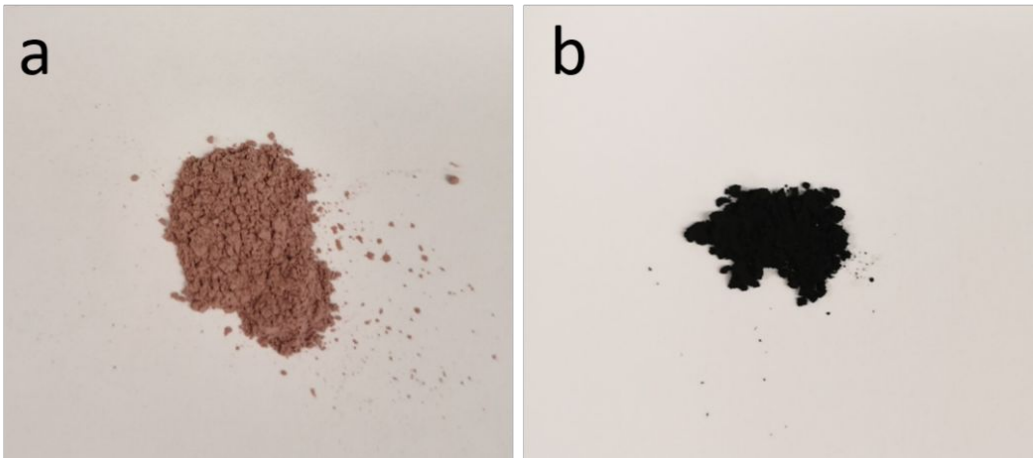

Figure S1. Photographs of (a) the $CoC_2O_4 \cdot 2H_2O$ precursor and (b) a Co_3O_4-400 sample.

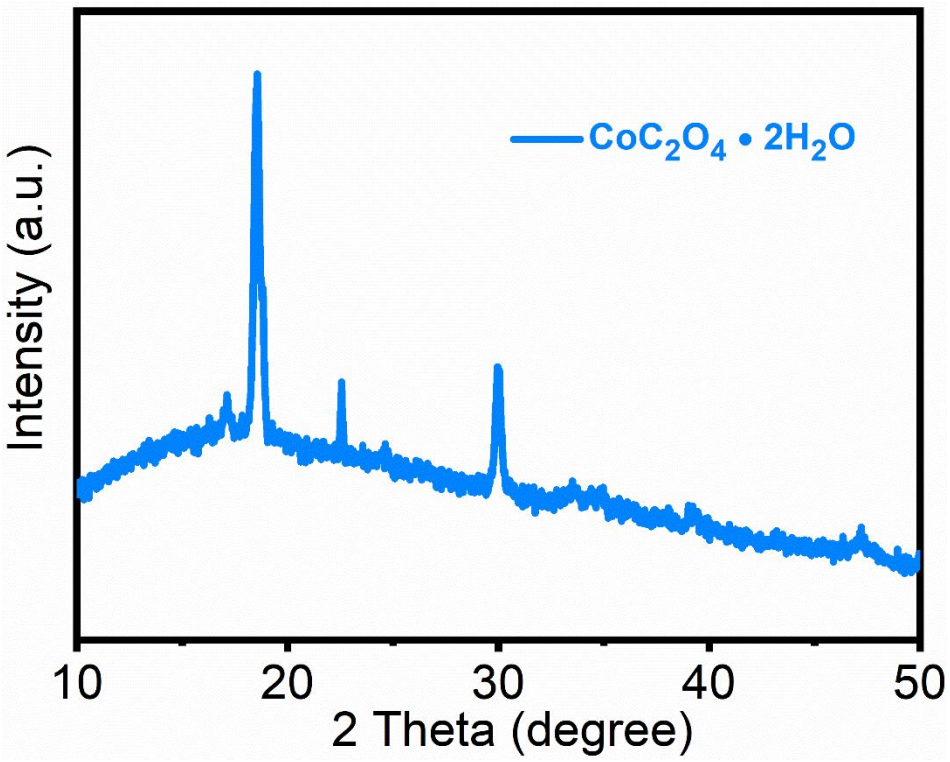

Figure S2. XRD pattern of the $CoC_2O_4 \cdot 2H_2O$ precursor.

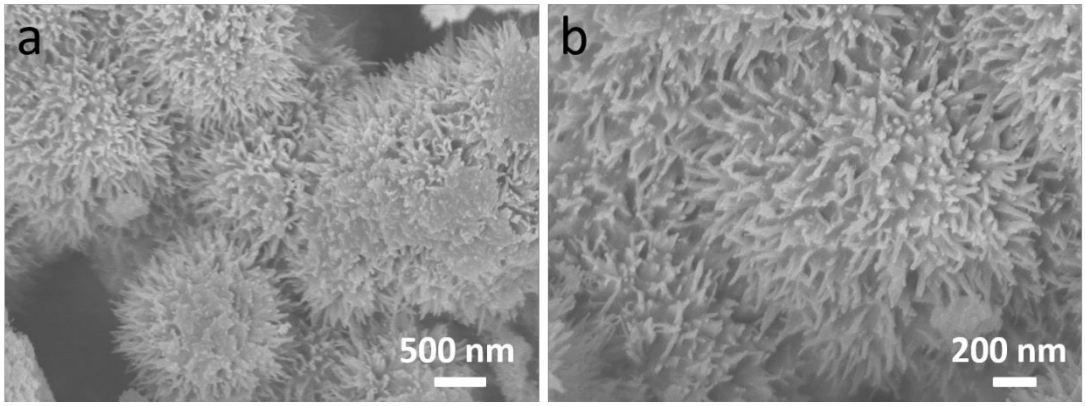

Figure S3. (a) Low-magnification and (b) high-magnification SEM images of the $CoC_2O_4 \cdot 2H_2O$ precursor.

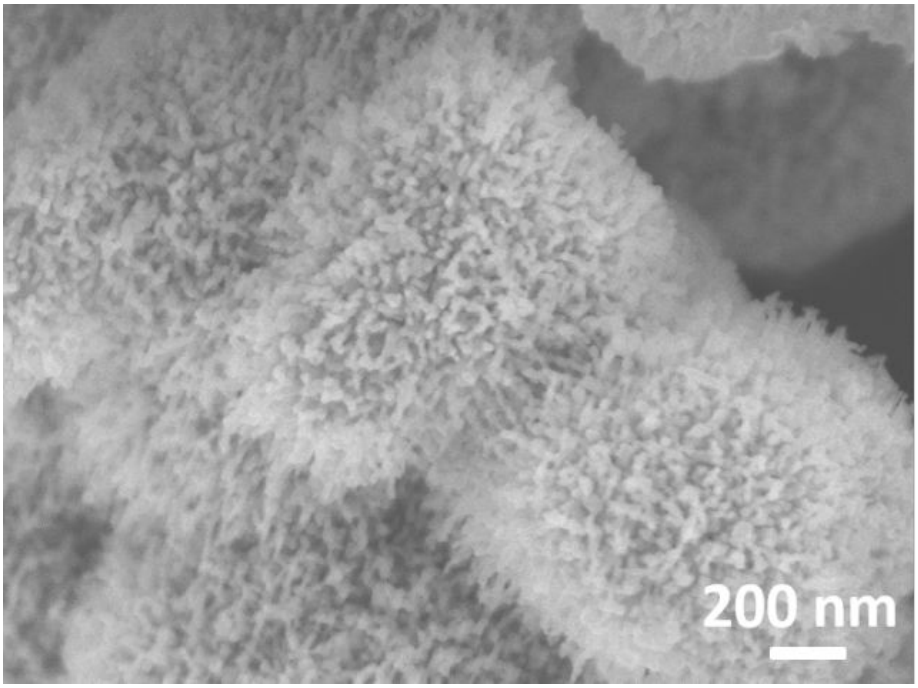

Figure S4. A high-magnification SEM image of Co_3O_4-400.

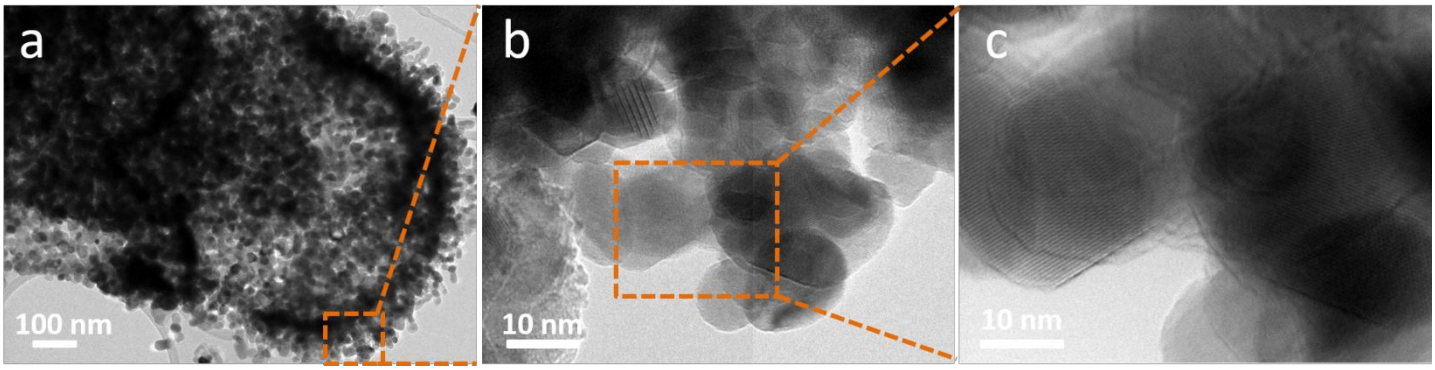

Figure S5. (a-c) TEM images of Co_3O_4-400 with different magnifications.

Table S1. The O1, O2, and O3 contents of the different Co_3O_4 samples from XPS analysis.

	O1 (at%)	O2 (at%)	O3 (at%)
Co_3O_4-400	41.77	45.15	13.08
Co_3O_4-800	57.48	33.02	9.50

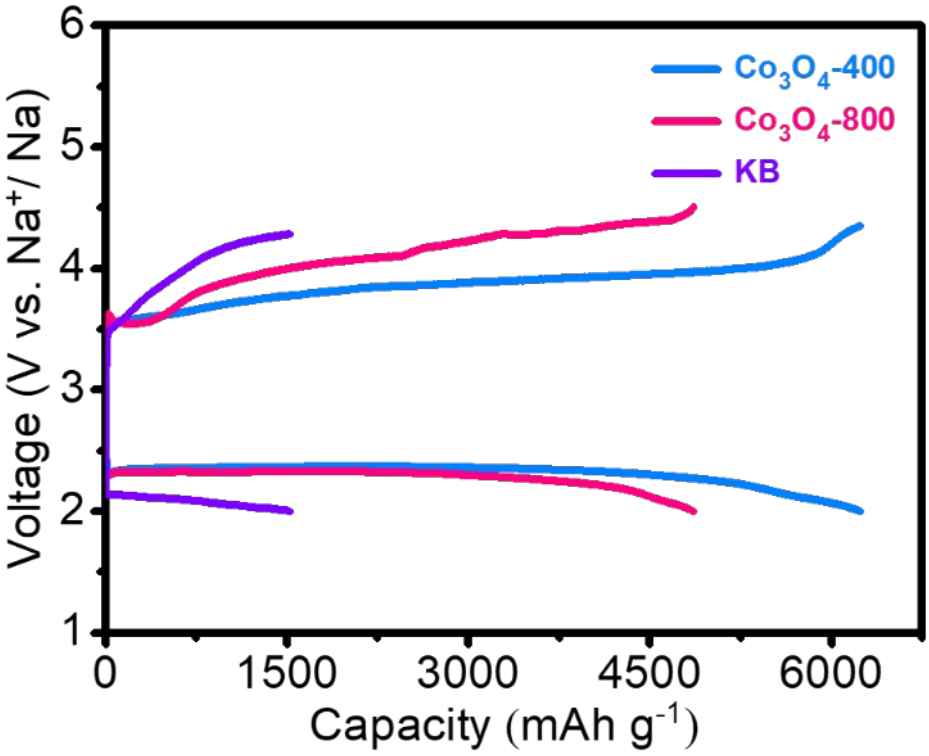

Figure S6. Full discharge/charge profiles of Na-CO_2 batteries with Co_3O_4-400, Co_3O_4-800, and KB cathodes tested at 100 mA g^{-1} within the voltage range of 2.0 to 4.8 V.

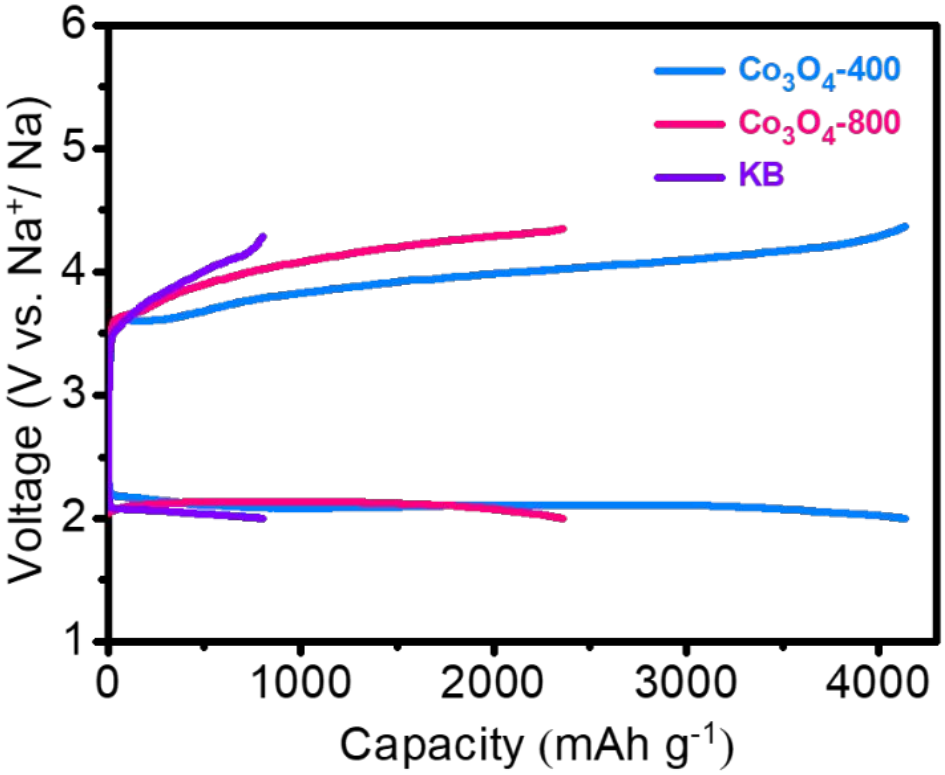

Figure S7. Full discharge/charge profiles of Na-CO_2 batteries with Co_3O_4-400, Co_3O_4-800, and KB cathodes tested at 200 mA g^{-1} within the voltage range of 2.0 to 4.8 V.

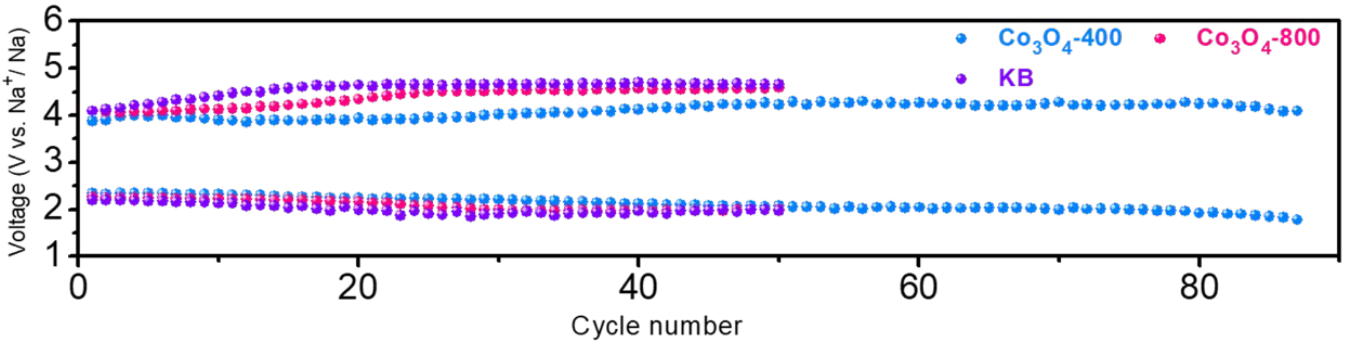

Figure S8. The terminal discharging and charging voltage profiles of Na-CO_2 batteries with Co_3O_4-400, Co_3O_4-800, and KB cathodes at the current density of 100 mA g^{-1}.

Table S2. Full discharge-charge and cycle performance of different materials for nonaqueous rechargeable Na-CO_2 batteries.

	Full discharge-charge			Cycle performance					
Cathode	Current density (mA g^{-1})	Discharge Capacity (mAh g^{-1})	Overp-otential (V) *	Current density (mA g^{-1})	Cut-off Capacity (mAh g^{-1})	Terminal voltage gap of the 1st cycle (V) *	Terminal voltage gap of the last cycle (V) *	Cycle performance	Ref.
Co_3O_4 with oxygen-vacancy	50	8371.3	**1.53**	100	500	1.55	2.31	87	This work
	100	6237.4	**1.53**						
	200	4136.8	**1.88**						
Ru/CNT	100	20 277	**~ 1.70**	100	500	~ 1.20	~ 1.85	100	1
$ZnCo_2O_4$@CNT	100	12 475	**~ 1.65**	100	500	~ 2.10	~ 2.50	150	2
Ru@KB	100	11537	**~ 2.00**	200	1000	~ 1.50	~ 2.00	130	3
Co_2MnO_x	200	8848	**~ 1.90**	N/A	500	~ 1.95	~ 2.00	75	4
Na_2CO_3 and CNTs	N/A	N/A	N/A	0.05 mA cm^{-2}	0.3 mAh cm^{-2}	~ 1.60	~ 2.00	100	5
t-MWCNT	1000	60 000	**~ 2.00**	1000	1000	0.60	1.30	200	6
MoS_2/SnS_2	50	35 889	N/A	50	500	~ 1.95	~ 1.60	100	7
γ-MnO_2	100	7286	**~ 1.60**	100	1000	~ 1.40	~ 1.50	50	8

RuO_2 nanoparticles encapsulated in carbon paper	0.1 mA cm^{-2}	2.788 mAh cm^{-2}	**~ 1.80**	0.1 mA cm^{-2}	0.1 mAh cm^{-2}	~ 1.80	~ 2.30	> 350	9
RuO_2@a-MWCNTs	N/A	N/A	N/A	100	500	~ 1.60	~ 2.00	~120	10
Cobalt-decorated carbon nanofibers	100	5714.3	N/A	100	200	~ 2.00	N/A	128	11

*These values were obtained by directly reading the data from the discharge-recharge curves in the paper.

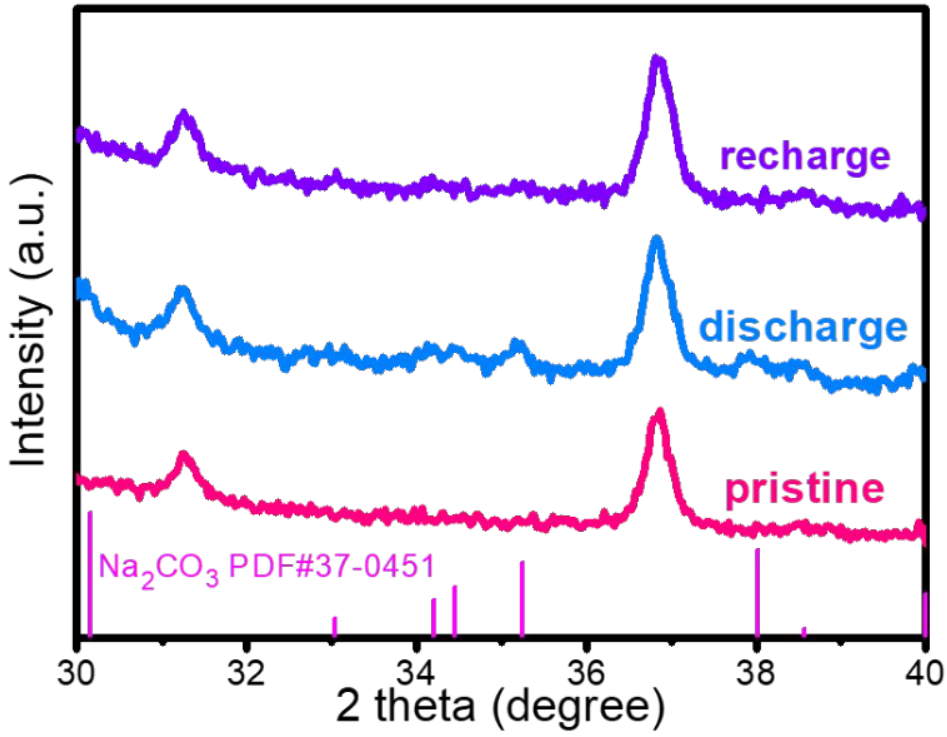

Figure S9. XRD patterns of the Co_3O_4-400 cathode in different states.

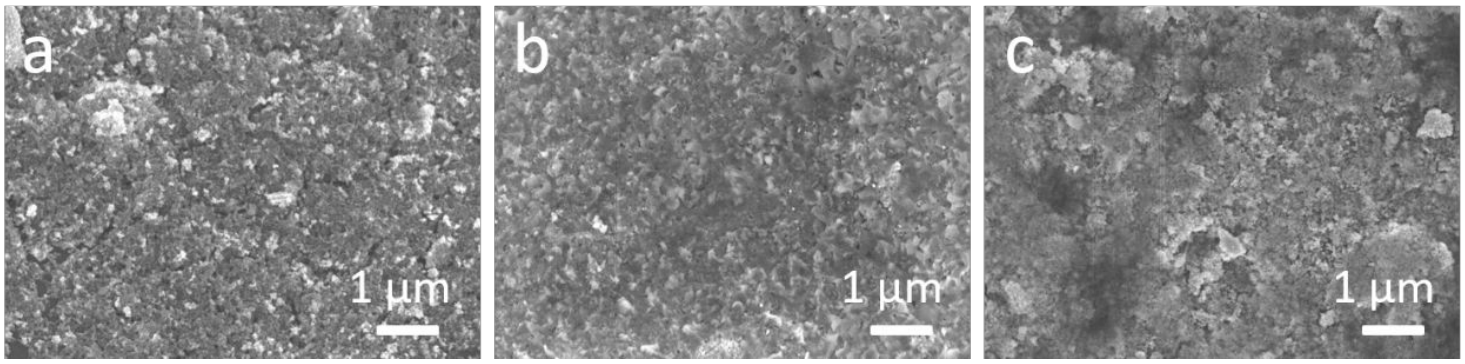

Figure S10. Low-magnification SEM images of the Co_3O_4-400 cathode surface: (a) before cycling, (b) after the first discharge, and (c) after the first recharge.

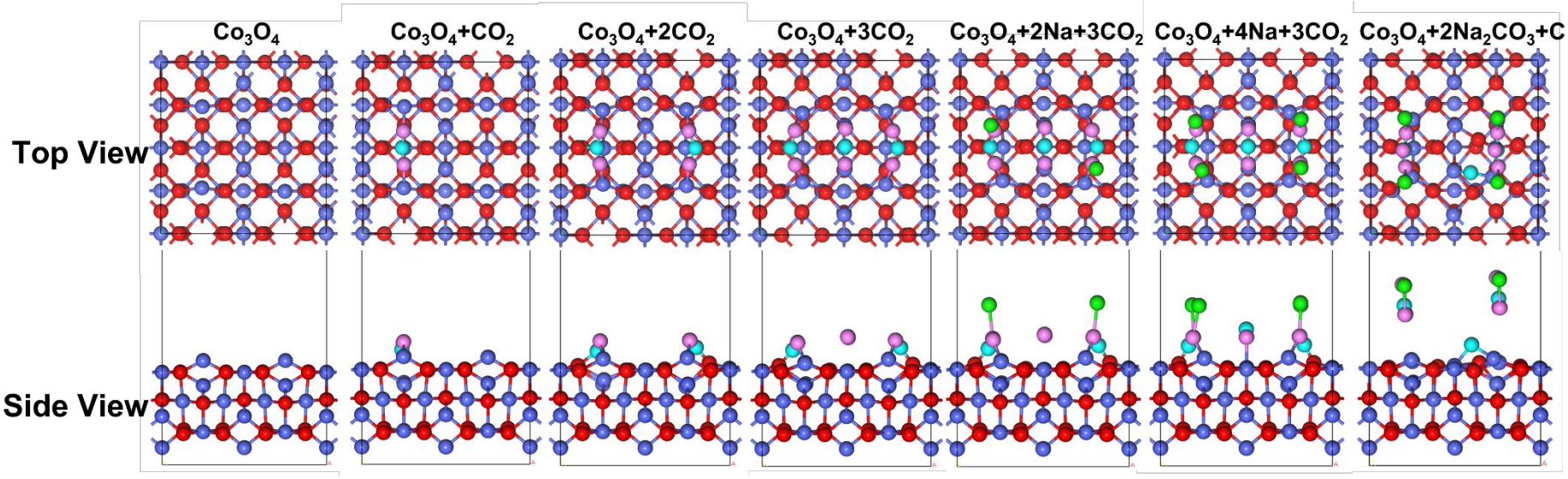

Figure S11. Configurations of CO_2 gas adsorption sites and Na_2CO_3 formation sites on the Co_3O_4 (0 0 1) surface (Co_3O_4: red: Co, light purple: O. CO_2 and Na_2CO_3: light blue: C, pink: O, green: Na).

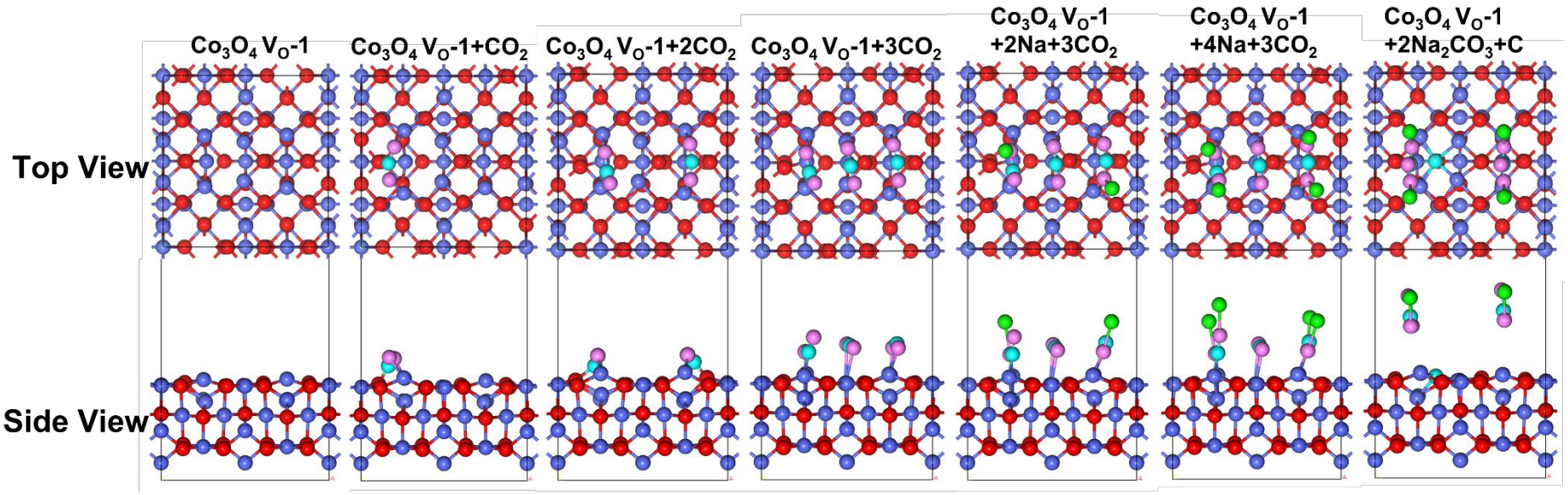

Figure S12. Configurations of CO_2 gas adsorption sites and Na_2CO_3 formation sites on the Co_3O_4 (0 0 1) surface with oxygen vacancies (Co_3O_4: red: Co, light purple: O. CO_2 and Na_2CO_3: light blue: C, pink: O, green: Na).

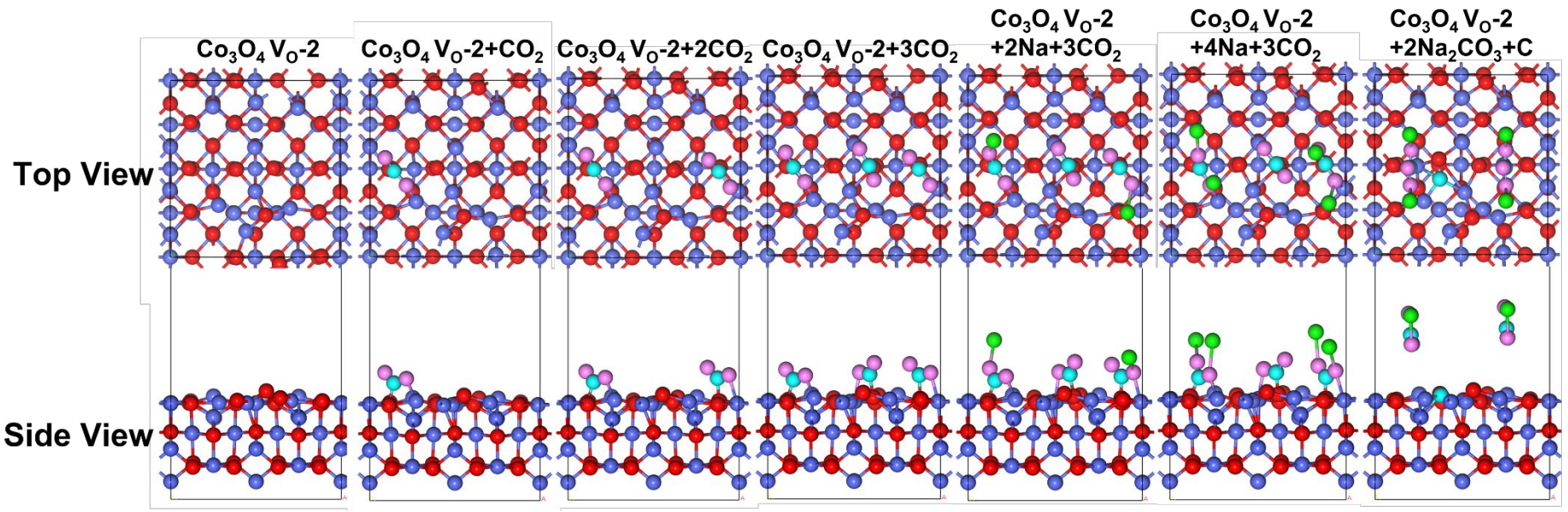

Figure S13. Configurations of CO_2 gas adsorption sites and Na_2CO_3 formation sites on the Co_3O_4 (0 0 1) surface with oxygen vacancies (Co_3O_4: red: Co, light purple: O. CO_2 and Na_2CO_3: light blue: C, pink: O, green: Na).

Table S3. The adsorption energy of CO_2 and sodium carbonate on Co_3O_4 (0 0 1) and Co_3O_4 (0 0 1) with oxygen vacancies. (Unit: eV)

Structures	Co_3O_4	Co_3O_4 (0 0 1) V_O-1	Co_3O_4 (0 0 1) V_O-2
CO_2	-0.883	-1.096	-0.982
$2CO_2$	-1.694	-1.932	-1.833
$3CO_2$	-2.407	-2.543	-2.472
$3CO_2 + 2Na$	-2.904	-3.001	-2.956
$3CO_2 + 4Na$	-2.245	-2.434	-2.349
$2Na_2CO_3 + C$	-1.410	-1.865	-1.736

References:

(1) Thoka, S.; Tsai, C. M.; Tong, Z. Z.; Jena, A.; Wang, F. M.; Hsu, C. C.; Chang, H.; Hu, S. F.; Liu, R. S. Comparative Study of Li-CO_2 and Na-CO_2 Batteries with Ru@CNT as a Cathode Catalyst. *ACS Appl. Mater. Interfaces* **2021**, *13* (1), 480-490.

(2) Thoka, S.; Tong, Z. Z.; Jena, A.; Hung, T. F.; Wu, C. C.; Chang, W. S.; Wang, F. M.; Wang, X. C.; Yin, L. C.; Chang, H.; Hu, S. F.; Liu, R. S. High-Performance Na-CO_2 Batteries with $ZnCo_2O_4$@CNT as the Cathode Catalyst. *J. Mater. Chem. A* **2020**, *8* (45), 23974-23982.

(3) Guo, L. N.; Li, B.; Thirumal, V.; Song, J. X. Advanced Rechargeable Na-CO_2 Batteries Enabled by a Ruthenium@Porous Carbon Composite Cathode with Enhanced Na_2CO_3 Reversibility. *Chem. Commun.* **2019**, *55* (55), 7946-7949.

(4) Fang, C.; Luo, J. M.; Jin, C. B.; Yuan, H. D.; Sheng, O. W.; Huang, H.; Gan, Y. P.; Xia, Y.; Liang, C.; Zhang, J.; Zhang, W. K.; Tao, X. Y. Enhancing Catalyzed Decomposition of Na_2CO_3 with Co_2MnO_x Nanowire-Decorated Carbon Fibers for Advanced Na-CO_2 Batteries. *ACS Appl. Mater. Interfaces* **2018**, *10* (20), 17240-17248.

(5) Sun, J. C.; Lu, Y.; Yang, H.; Han, M.; Shao, L. Y.; Chen, J. Rechargeable Na-CO_2 Batteries Starting from Cathode of Na_2CO_3 and Carbon Nanotubes. *Research* **2018**, *2018*, 6914626.

(6) Hu, X. F.; Sun, J. C.; Li, Z. F.; Zhao, Q.; Chen, C. C.; Chen, J. Rechargeable Room-Temperature Na-CO_2 Batteries. *Angew. Chem., Int. Ed.* **2016**, *55* (22), 6482-6486.

(7) Pichaimuthu, K.; Jena, A.; Chang, H.; Su, C. C.; Hu, S. F.; Liu, R. S. Molybdenum Disulfide/Tin Disulfide Ultrathin Nanosheets as Cathodes for Sodium-Carbon Dioxide Batteries. *ACS Appl. Mater. Interfaces* **2022**, *14* (4), 5834-5842.

(8) Chen, X. Y.; Chen, J.; Liu, Y. J.; Liu, Y.; Gao, Y.; Fan, S. W.; He, X. X.; Liu, X. H.; Shen, C.; Jiang, Y.; Li, L.; Qiao, Y.; Chou, S. L. Advanced Li/Na-CO_2 Batteries Enabled by the γ-MnO_2 Catalyst with Enhanced Carbonate Decomposition. *ACS Appl. Mater. Interfaces* **2023**, *15* (23), 28106-28115.

(9) Xu, C. F.; Qiu, J. J.; Dong, Y. L.; Li, Y. L.; Shen, Y. L.; Zhao, H. P.; Kaiser, U.; Shao, G. S.; Lei, Y. Dual-Functional Electrode Promoting Dendrite-Free and CO_2

Utilization Enabled High-Reversible Symmetric Na-CO_2 Batteries. *Energy Environ. Mater.* **2023**, 0, e12626.

(10) Wang, Z. Z.; Cai, Y. C.; Ni, Y. X.; Lu, Y.; Lin, L.; Sun, H. X.; Li, H. X.; Yan, Z. H.; Zhao, Q.; Chen, J. Ultrafine RuO_2 Nanoparticles/MWCNTs Cathodes for Rechargeable Na-CO_2 Batteries with Accelerated Kinetics of Na_2CO_3 Decomposition. *Chinese Chem. Lett.* **2023**, *34* (3), 107405.

(11) Tang, M.; Du, J. Y.; Ma, J. L.; Wang, X. D.; Zhang, X.; Shen, Q. Y.; Wang, F. P.; Wang, Y. Cobalt-Decorated Carbon Nanofibers as a Low Overpotential Cathode for Nonaqueous Na-CO_2 Batteries. *J. Alloy Compd.* **2022**, *911*, 165054.